Published in final edited form as:
Prostate. 2014 September ; 74(13): 1308–1319. doi:10.1002/pros.22847.

Pharmacokinetics and Toxicology of a Fibroblast Activation Protein (FAP)-activated Prodrug in Murine Xenograft Models of Human Cancer

W. Nathaniel Brennen[1,2], **D. Marc Rosen**[1,2], **Alcides Chaux**[2,3], **George J. Netto**[2,3], **John T. Isaacs**[1,2], and **Samuel R. Denmeade**[1,2]

[1]Chemical Therapeutics Program, The Sidney Kimmel Comprehensive Cancer Center at Johns Hopkins, The Johns Hopkins University School of Medicine, Baltimore, MD 21287

[2]Department of Oncology, The Sidney Kimmel Comprehensive Cancer Center at Johns Hopkins, The Johns Hopkins University School of Medicine, Baltimore, MD 21287

[3]Department of Pathology, The Sidney Kimmel Comprehensive Cancer Center at Johns Hopkins, The Johns Hopkins University School of Medicine, Baltimore, MD 21287

Abstract

Background—As carcinoma progresses, the stroma undergoes a variety of phenotypic changes, including the presence of carcinoma-associated fibroblasts (CAFs) that express fibroblast activation protein (FAP). FAP is a post-prolyl endopeptidase whose expression in a healthy adult is largely restricted to the cancer-associated stroma. FAP-targeted prodrugs with a 100-fold greater therapeutic window over the parent compound were previously generated.

Methods—Prodrugs and non-cleavable controls were incubated in the presence of FAP. Plasma and tumor half-lives ($t_{1/2}$) of the full-length and active forms of the prodrugs were determined using LCMS. Biodistribution studies of prodrug activation were performed. Histopathological analysis of tissues from treated animals were compared to vehicle-treated controls. Toxicity and efficacy studies were performed in human breast (MDA-MB-231 and MCF-7) and prostate (LNCaP) cancer xenografts models.

Results—These FAP-activated prodrugs have a significantly slower clearance from tumor tissue than the circulation (~12 vs. ~4.5 hrs). Micromolar concentrations of active drug persist in the tumor. Active drug is detected in non-target tissues; however, histopathologic evaluation reveals no evidence of drug-induced toxicity. A FAP-activated prodrug (ERGETGP-S12ADT) inhibits tumor growth in multiple human breast and prostate cancer xenograft models. The anti-tumor effect is comparable to that observed with docetaxel, but results in significantly less toxicity.

Conclusion—FAP-activated prodrugs are a viable strategy for the management of prostate and other cancers. These prodrugs exhibit less toxicity than a commonly used chemotherapeutic agent. Further refinement of the FAP cleavage site for greater specificity may reduce prodrug activation in non-target tissues and enhance clinical benefit.

Corresponding Author: W. Nathaniel Brennen, 1650 Orleans St., CRB-I, Rm 162B, Baltimore, MD 21287, wbrenne2@jhmi.edu, Phone: (410) 502-6814, Fax: (410) 614 - 8397.

Keywords

fibroblast activation protein; FAP; prodrug; carcinoma-associated fibroblast; CAF; pharmacokinetics

Introduction

Cancer continues to be a devastating disease responsible for the deaths of millions of people world-wide. Tumor heterogeneity resulting from genomic instability leads to ready-made 'escape mutants' resistant to targeted therapy with alarming frequency (1). This fact justifies the need for novel therapies that are able to kill cancer cells independent of ubiquitous target expression. One promising approach is the development of tumor- or tissue-specific protease-activated prodrugs, or 'molecular grenades' (2). This approach entails conjugating a cytotoxic compound to a peptide sequence containing a cleavage site selectively recognized by a tissue- or tumor-specific protease of choice (3). Hydrolysis of the peptide bond at the engineered cleavage site results in liberation of the toxin or drug in its bioactive form in the extracellular fluid, which then targets adjacent cells through a bystander effect. Importantly, this strategy allows us to give higher therapeutic doses resulting in increased clinical efficacy while minimizing the dose-limiting toxicities (DLTs) associated with systemic administration of traditional chemotherapeutics. Our laboratory has previously developed prodrugs targeting Prostate-Specific Antigen (PSA), human Kallikrein 2 (hK2) and Prostate-Specific Membrane Antigen (PSMA) (3–6). A bacterial protoxin targeting Prostate-Specific Antigen (PSA) has completed Phase I and II clinical trials for the treatment of localized prostate cancer and benign prostatic hyperplasia (BPH) (7–8). Phase I trials evaluating a Prostate-Specific Membrane Antigen (PSMA)–activated prodrug as a therapy for metastatic cancer have also been completed (6).

More recently, we have designed and developed a Fibroblast Activation Protein (FAP)-activated prodrug (9). FAP is a type II integral membrane serine protease expressed on the surface of carcinoma-associated fibroblasts (CAFs) in the stroma of greater than 90% of solid tumors examined, but not on adjacent normal tissues (10–13). FAP expression has also been observed on activated fibroblasts in some soft tissue sarcomas and at sites of active tissue remodeling, including areas of wound healing, rheumatoid arthritis, and chronic fibrosis (10–11,13–15). Mesenchymal stem cells (MSCs), which can give rise to CAFs, and tumor-associated macrophages (TAMs) have also been shown to express FAP. (10,16–17). Both of these cell types have significant immunomodulatory properties that may play critical roles in tumor progression (16,18). This is supported by studies in which conditional knockout of FAP-expressing cells using diphtheria toxin restored immunological control of tumor growth in a genetically-engineered mouse model of pancreatic cancer (19).

FAP is a member of the dipeptidyl peptidase subfamily whose members are characterized by the ability to cleave the peptide bond following a proline residue (10,20). Like all members of the family, FAP is a dipeptidase (10,20). Unique to FAP among the family is its endopeptidase activity, which allows it to cleave internal peptide bonds in large molecules like collagen I (21–22). Motivated by this distinct enzymatic activity and largely tumor-

restricted expression pattern to develop a FAP-activated prodrug, we probed the extended substrate specificity through mapping FAP cleavage sites within gelatin derived from human collagen I (21). Several FAP-selective cleavage sequences were identified and hydrolysis kinetics were characterized. The top candidates were selected to design FAP-activated prodrugs incorporating a thapsigargin (TG)-amino acid analog, amino acid-8-O-12-aminododecanoyl)-8-O-debutanoylthapsi-gargin (aa12ADT), as the cytotoxic 'warhead' (Fig. 1A) (23–25). The aa12ADT analogs, which comprise the active portion of the drug, have previously been shown to retain their low nanomolar potency (9,25–27). These FAP-activated prodrugs were shown to be well-tolerated with no obvious toxicity to the host and exhibited significant efficacy against both breast and prostate human cancer xenografts (9). Tumors treated with these FAP-activated prodrugs displayed stromal-selective cell death based upon immunocytochemical analysis. Evidence of a bystander effect leading to the death of adjacent cell populations within the tumor, including pericytes, endothelial cells, and malignant epithelium was also apparent. Most significantly, we were able to demonstrate a 100-fold increase in the therapeutic window between the active compound (aa12ADT) and the full-length prodrug form (9).

To further clarify the basis for this increase in the therapeutic window, we examined the pharmacokinetics and biodistribution of FAP prodrug activation in both tumor-bearing and naïve mice. The mouse genome encodes a homolog of FAP (mFAP) that shares 89% sequence identity with its human counterpart including the catalytic triad (10). Similar to the human expression pattern, mFAP is expressed on activated fibroblasts in areas of tissue remodeling such as the tumor microenvironment and wound healing, but not in adjacent normal tissues (28–29). A soluble, extracellular form of FAP has been detected in the plasma of both humans and mice by our group and others (9,30). However, the amount of FAP activity present in the plasma is distinct between the two species with the mouse having ~10-fold higher levels than is present in human plasma (9). The comparable expression pattern and increased plasma activity make the mouse a suitable, but extremely rigorous model for testing the safety of administering a FAP-activated prodrug. The importance of which is highlighted by recent preclinical studies suggesting that elimination of FAP-positive cells can lead to cachexia and anemia in mice (31–32).

Here we report that our lead FAP-activated prodrug, ERGETGP-S12ADT, accumulates to low micromolar (μM) levels in tumor tissue and is cleared at a significantly lower rate from the tumor than it is from plasma (~12 vs. 4.5 hrs). By comparing the amount of active drug (S12ADT) produced to that generated from a series of non-FAP cleavable prodrug analogs, we have demonstrated that activation may be as much as 80–90% specific for FAP activity. The active form of the drug is also detected in non-target tissues; however, histopathologic analysis demonstrated no drug-induced toxicity. The greatest accumulation of active drug is observed in the tumor, which leads to a significant inhibition of tumor growth in multiple xenograft models of human breast and prostate cancer.

Materials and Methods

Reagents

DMEM, RPMI-1640, L-glutamine, penicillin-streptomycin, phosphate-buffered saline (PBS), fetal bovine serum (FBS) and heat-inactivated FBS were all obtained from Invitrogen (Carlsbad, CA). Boc-protected 12-aminododecanoyl thapsigargin (Boc-12ADT) was provided as a gift by Dr. Soeren Christensen, University of Copenhagen, Denmark. 12ADT-conjugated peptide prodrugs were produced by California Peptide Research (Napa, CA) according to previously described methods (4). FAP was expressed recombinantly in Schneider's S2 cells and purified from the culture supernatant as previously described (21).

Cell Lines

Human LNCaP prostate cancer and MCF-7 breast cancer cell lines were obtained from ATCC (Manassas, VA). LNCaP cells were grown as a monolayer in RPMI-1640 supplemented with 10% FBS, 1% L-Glutamine, and 1% Pen/Strep at 37°C in a humidified incubator with 5% CO_2. MCF-7 cells were grown in an analogous manner using DMEM media. Schneider's S2 (Invitrogen, Carlsbad, CA) cells were grown as a suspension culture at room temperature in DES medium (Invitrogen) supplemented with heat-inactivated FBS.

FAP-mediated Hydrolysis of Prodrugs ex vivo

Prodrugs ([1μM] final concentration) were added to FAP buffer (100mM NaCl, 100mM Tris, pH 7.8). All samples contained 10% DMSO and were incubated at 37°C for 24hrs in a shaking incubator +/− 200nM FAP. Prodrug hydrolysis was monitored by high pressure liquid chromatography/quadripole mass spectroscopy (LCMS) detection of the active forms of the drugs (A-, S-, E-12ADT) at 0, 4 and 24hrs.

Hydrolysis of Prodrugs in Plasma ex vivo

Prodrugs ([100 μM] final concentration) were added to plasma obtained from intra-cardiac puncture of fully anesthetized mice. Samples were incubated at 37°C for 24 hrs in a shaking incubator. Prodrug hydrolysis was monitored by LCMS detection of the active forms of the drugs (A-, S-, E-12ADT) at 0 and 24hrs.

Determination of Plasma and Tissue Levels of FAP Prodrugs

Heparinized plasma samples from mice treated with FAP prodrugs and control plasma from naïve mice were obtained by cardiac puncture of anesthetized mice. A series of calibration standards (100pM – 100 μM)for each of the FAP prodrugs and active drugs (A12ADT, E12ADT, S12ADT, and 12ADT) were made using 50% acetonitrile/water containing 0.1% formic acid (FA). The internal standard (IS), L12ADT, was diluted to 1 μM using the same solvent. All samples were deproteinated using 100% acetonitrile containing 0.1% FA, vortexed, and centrifuged at 15,000 RPM for 5 minutes. The resulting supernatant was transferred to an autosampler vial for injection into the LCMS.

The analytical system consists of a binary gradient HPLC system and automatic sampler (Perkin Elmer, Waltham, MA). The mobile phase is composed of 5% Acetonitrile/water/ 0.1% FA (Solv A) and 100% Acetonitrile/0.1% FA (Solv B). The initial conditions are 60%

Solv A / 40% Solv B at a flow rate of 0.25 mL/min. The injection volume is 10 μL and the separation is carried out in a 100×2 mm, 2.5 μm reversed phase HPLC column (Phenomenex Luna, Torrance, CA) At 1 minute following injection a linear gradient raises the mobile phase composition to 100% Solv B at 7 minutes with a return to initial conditions at 9 minutes. The turbo ion spray voltage was set at 5000 v and drying gas heated to 450°C was used for desolvation. Detection was carried out by a triple quadrapole mass spectrometer (Applied Biosystems ABI 3000, Carlsbad, CA) in the positive mode using multiple reaction monitoring to detect and discriminate compounds based on their precursor ion and product ion transitional pairs. Linear regression analysis was used to generate best-fit lines, from which peak areas of samples were converted to concentration of the full-length FAP prodrug or free drugs. The terminal half-life ($t_{1/2}$) was determined from the terminal slope (k_e) on a log-linear plot of concentration versus time.

In vivo Assays: Tumor xenograft studies and Tissue toxicity

Mouse care and treatment was approved by and performed in accordance with the guidelines of the Animal Care and Use Committee of the Johns Hopkins University School of Medicine. For efficacy studies, suspended tumor cells were placed in a 60% mixture of Matrigel Matrix (BD Biosciences, San Jose, CA) in HBSS at a concentration of 2.0×10^6 cells per 100 μL of solution. LNCaP cells were then injected subcutaneously into the rear flanks of 6wk old male nude mice (n = 10/group). MCF-7 cells were injected subcutaneously into 6 wk old female nude mice (n = 10/group) previously implanted subcutaneously with a slow release estrogen pellet (0.72 mg of 17β-estradiol; Innovative Research of America, Sarasota, FL) in the contralateral flank. Ten mice were treated per group. Animals treated with a FAP-activated prodrug received 6.8 mg/kg/dose (10 nmoles) IV on days 0, 1, and 2 for 1–3 cycles as indicated for each experiment. Animals treated with docetaxel received 12 mg/kg/dose (4 nmoles) IV on days 0, 3, and 6 for a single cycle. Weekly tumor measurements were made with calipers and the tumor volume (cm^3) was calculated ($0.5236 \times L \times W \times H$).

For the histopathological examination, mice received 3 daily IV doses of the FAP-activated ERGETGP-S12ADT prodrug at 6.8 mg/kg. Mice were euthanized via CO_2 overdose at 20 days post-therapy and tissues were harvested, weighted and processed for immunohistochemical analysis as previously described (4). Briefly, tissues and tumors were fixed in a 10% formalin solution in PBS and embedded in paraffin prior to staining with hemotoxylin-eosin (H&E) using standard methods. Tissues from prodrug- and vehicle-treated controls were examined by two pathologists for gross morphological or cellular abnormalities in a blinded fashion.

Statistical Analysis

All statistics were performed using Microsoft Excel software. *P* values were calculated using a Student's *t* test and values < 0.05 were considered statistically significant. All statistical analyses were paired and two-sided. All error bars represent +/− standard error (SE) and were calculated by dividing the standard deviation (SD) by the square root of the sample size (n).

Results

Characterization of FAP-activated Prodrugs and Controls

The active form of the drugs (S- or A12ADT, respectively) are generated from the ERGETGP-S12ADT and ASGPAGP-A12ADT prodrugs in the presence of FAP *in vitro* (Fig. 1B), but are completely stable in its absence (data not shown). Consistent with the previously reported hydrolysis kinetics (21), the ERGETGP-S12ADT prodrug released ~15-fold more active drug than the ASGPAGP-A12ADT prodrug (30 vs. 2 μM, respectively). Three 'prodrug controls' were generated based upon this lead prodrug sequence (Fig. 1A). The first converted the proline in the P1 position of the cleavage site to a *D*-amino acid (ERGETGp-S12ADT, where p represents the *D*-isomer of proline). The second and third were designed with a scrambled version of the cleavage sequence (PETGRSG-E12ADT) with one incorporating a morpholino (μ) cap to protect the NH_2-terminus from aminopeptidase degradation and one left unprotected. These 'prodrug controls' were resistant to FAP cleavage (Fig. 1B).

Pharmacokinetics of FAP-activated Prodrugs and non-FAP Cleavable Controls

The half-life ($t_{1/2}$) of the ERGETGP-S12ADT and ERGETGp-S12ADT prodrugs in mouse plasma are ~4–5 hrs following a single intravenous (IV) dose with the FAP-activated prodrug being cleared slightly faster (Fig. 2A). The prodrugs reach a peak concentration (C_{max}) of ~35–40 μM within 1 hr of dosing and are almost entirely cleared from circulation by 24 hrs post-infusion. Less than 1% of the administered dose is converted to the active form in the plasma of mice treated with the FAP-activated ERGETGP-S12ADT prodrug (Fig. 2B). S12ADT appears to be further processed as an intermediate to the 12ADT parent compound. Therefore, the total active drug generated from the prodrug comprises both the S- and 12ADT forms. In contrast, no measurable S12ADT is generated in mouse plasma from the non-FAP cleavable ERGETGp-S12ADT *D*-isomer prodrug (Fig. 2C). The 12ADT parent compound is detected in mouse plasma following IV dosing with the *D*-isomer prodrug control; however, these levels were <0.01% of the total administered dose.

The prodrugs are cleared at a significantly slower rate once they reach the tumor with half-lives in excess of 12 hrs (Fig. 3). The active form of the drug accumulates in tumors and reaches concentrations in the low micromolar range (2 μM) within 24 hrs following a single IV dose of the FAP-activated prodrug, ERGETGP-S12ADT (Fig. 3A). Active drug concentrations in the tumor increase to ~3–5 μM following three doses of the FAP-activated prodrugs over three days (Fig. 3C). Micromolar (μM) levels of active form of the drug persist in the tumors of animals treated with a FAP-activated prodrug for at least five days following cessation of therapy (Fig. 3D). In contrast, the non-FAP cleavable *D*-isomer prodrug control continues to accumulate in tumor tissue in an inactive form during the first 4 hrs post-injection (Fig. 3B) consistent with a slower rate of processing. The non-FAP cleavable prodrug is then cleared from tumor tissue with a half-life of ~16 hrs. Active drug concentrations in tumors treated with the non-FAP cleavable *D*-isomer prodrug control are approximately 7-fold lower than those achieved with the FAP-activated ERGETGP-S12ADT prodrug (Fig. 3). Consistent with non-FAP mediated activation, these levels are

almost entirely comprised of 12ADT in animals treated with the *D*-isomer prodrug control (Fig. 3B).

Biodistribution of FAP-selective Prodrug Activation

To address the specificity of FAP prodrug activation we compared the biodistribution of the active drug produced from the FAP cleavable prodrugs to that from the non-FAP cleavable *D*-isomer control. As previously stated, active drug levels of ~2 μM were measured in MCF-7 tumors from animals treated with a single IV dose of the FAP-activated ERGETGP-S12ADT prodrug at 24 hrs post-infusion (Fig. 3C). This is nearly four times greater accumulation than is achieved with the ASGPAGP-A12ADT FAP-activated prodrug and seven-fold more than is produced from the non-FAP cleavable *D*-isomer prodrug control (Fig. 4A).

While the greatest accumulation of active drug is observed in the tumor, there are also significant levels present in other tissues. The liver and kidneys contain elevated levels of active drug as expected from their roles in detoxification and clearance; however, active drug is also detected in other tissues, including the heart (Fig. 4A). In all tissues examined, active drug concentrations are significantly higher in mice treated with the ERGETGP-S12ADT prodrug compared to those treated with the ERGETGp-S12ADT *D*-isomer control. There are no significant differences observed in active drug concentrations present in tissues from naïve and tumor-bearing animals treated with the ERGETGP-S12ADT prodrug (Fig. 4B), suggesting the presence of active drug in non-target tissues is not due to redistribution following activation in the tumor.

Skeletal muscle was selected as a representative non-target tissue to further probe the specificity of prodrug activation by FAP. Active drug is detected in the skeletal muscle of animals treated with the *D*-isomer analog, in addition to those treated with the capped and uncapped scrambled prodrug controls (Fig. 4C). The concentration of active drug produced by the controls is ~10–20% of the amount detected in the skeletal muscle of animals treated with the FAP-activated ERGETGP-S12ADT prodrug (Fig. 4C), suggesting proteolysis is ≥80% FAP-specific.

FAP activity in the plasma has previously been reported (9,30). Consistent with these reports, active drug is released from the two FAP-activated prodrugs when incubated in mouse plasma *ex vivo* (Fig. 4D), but not in saline under the same conditions (data not shown). In contrast, there is no active drug generated from the *D*-isomer control over this same time period consistent with FAP as the activating protease in plasma (Fig. 4D). Active drug concentrations reach ~20 nM from the scrambled-capped analog and approximately 4-times that amount is produced from the uncapped version (Fig. 4D). This suggests that the levels of active drug detected in non-target tissues could be the result of prodrug activation in the plasma and subsequent distribution into tissues through the circulation.

Lack of Drug-induced Toxicity in Peripheral Tissues from Mice receiving a FAP-selective Prodrug

Due to the unexpected levels of active drug detected in non-target tissues we wanted to look for evidence of tissue toxicity. The heart, liver, lungs, kidneys, spleen, and brain of animals treated with three consecutive daily doses of the FAP-activated ERGETGP-S12ADT were analyzed for signs of drug-induced toxicity at 20 days post-treatment. Tissues were assessed for gross morphological alterations and necrosis, in addition to indications of toxicity directly related to the drug's mechanism of action, i.e. apoptotic cells. All tissues examined appeared normal by histopathological standards, and no significant differences could be detected in the tissues of treated vs. untreated animals when analyzed by two pathologists in a blinded fashion (Fig. 5A). The only notable finding was a small area of granulomatous inflammation with moderate perivascular inflammation marked by the presence of lymphocytes and macrophages in the lung of one treated animal (Fig. 5B). However, this is unlikely due to therapy as it only occurred in one animal and no signs of apoptotic bodies were present to indicate a thapsigargin-induced mechanism of action. This analysis supports our previous observations that the prodrugs are well-tolerated and no overt toxicity is apparent in treated animals (9).

In vivo Efficacy of FAP-selective Prodrugs against Breast Cancer Xenografts

Despite the presence of active drug in non-target tissues, a significant therapeutic effect has been demonstrated against both breast and prostate cancer xenograft models using the ASGPAGP-A12ADT and ERGETGP-S12ADT FAP-activated prodrugs (9). In these previous studies, animals were treated with three consecutive daily doses for 1–2 cycles with 11 days off between each cycle. No obvious toxicity was associated with therapy and no mortality was observed on this treatment regimen (9). These observations combined with the lack of tissue toxicity detected in the current histopathology study (Fig. 5A) justified dose intensification to achieve a more sustained therapeutic response. Reducing the time between cycles by one week had no apparent adverse effects (Fig. 6A). However, escalating the number of cycles from two to three on this same schedule resulted in a slight increase in mortality (1 of 10 animals) compared to vehicle-treated controls. Surviving animals treated with the FAP-activated ERGETGP-S12ADT prodrug displayed a significant anti-tumor effect against MCF-7 xenografts (Fig. 6B). The average tumor burden in animals bearing MDA-MB-231 xenografts was smaller in the treatment group; however, this difference was not statistically significant. The difference in efficacy against these two models could be due to differences in the cancer cells themselves or in the supporting stroma being targeted by the prodrug, either qualitatively or quantitatively. In support of the latter, the stroma represents a smaller proportion of the overall tumor in MDA-MB-231 xenografts compared to that observed in MCF-7 tumors (Fig. 6C).

In vivo Comparison of a FAP-activated Prodrug to Docetaxel: Toxicity and Efficacy

We next wanted to compare the efficacy and treatment-associated toxicity of a commonly used standard chemotherapeutic agent, such as docetaxel, to a FAP-activated prodrug. Significant efficacy was previously demonstrated against LNCaP human prostate cancer xenografts using a FAP-activated prodrug (9). In the current study, a comparable anti-tumor

effect against LNCaP xenografts is observed with both the ERGETGP-S12ADT FAP-activated prodrug and docetaxel using standard dosing regimens for both compounds (Fig. 7A). However, animals treated with docetaxel lost an average of ~30% of their total body weight following therapy and did not recover over the course of the experiment (Fig. 7C–D). This is in contrast to animals given the ERGETGP-S12ADT FAP-activated prodrug who lost <15% of their body weight post-treatment and recovered to pre-treatment levels within 1 week of dosing (Fig. 7C–D). Interestingly, LNCaP xenografts are not typically characterized by a large proportion of stroma by H&E staining either, but can have relatively thick stromal cords running sporadically throughout the tumor (Fig. 7B).

Discussion

Thapsigargin (TG) is a highly potent cytotoxic agent with a unique proliferation-independent mechanism of action; however, the complete lack of specificity that results from targeting an essential cellular process (i.e., calcium homeostasis) makes it unappealing for therapeutic purposes (3–4,33–34). Rather than discard an agent with interesting properties, these same characteristics can be exploited for clinical benefit by designing TG-based prodrugs to create a therapeutic window. A TG analog has previously been identified that not only retains its potency, but also includes a functional group that can be modified with a peptide sequence containing a protease-specific cleavage site (25–26,35). By targeting a protease with a tumor- or tissue-restricted expression pattern, a cytotoxic prodrug can be selectively delivered to a site of interest prior to activation; thereby, reducing the side effects associated with systemic delivery. This approach has previously been utilized to engineer multiple TG-based protease-selective prodrugs, including ones activated by PSA, hK2, PSMA, and most recently, FAP (3–6,9,23). The PSMA-activated version, G202, has passed FDA-approved toxicology and completed Phase I clinical testing (6).

Earlier studies demonstrated a 100-fold increase in the therapeutic window of a TG analog when administered in the form of a FAP-activated prodrug (9). A significant anti-tumor response against both human breast and prostate cancer xenograft models was observed with no associated toxicity (9). In contrast, TG has no therapeutic benefit when administered at the maximally-tolerated dose (MTD) (9). The current studies were performed in an effort to understand the mechanisms underlying the decreased toxicity of the TG analog when administered as a peptide-conjugated prodrug. These FAP-activated prodrugs have relatively short half-lives in plasma (4–5 hrs), but accumulate in tumor tissue over time (low μM) with a significantly slower rate of clearance once there ($t_{1/2}$ ≥12 hrs).

Given the lack of toxicity observed when administering these compounds systemically, a greater distribution of active drug was detected in non-target tissues than expected. Histopathological examination revealed no evidence of tissue damage at the macroscopic or cellular level following treatment with a FAP-activated prodrug. TG and the active forms of TG-based prodrugs are highly lipophilic and immediately sequestered in adjacent cells; thereby, preventing them from re-entering systemic circulation following activation. This was confirmed by experiments comparing active drug concentrations in non-target tissues from tumor-bearing and naïve mice demonstrating no differences in biodistribution.

An alternative explanation for the observed biodistribution may be the presence of FAP activity in the plasma (9,30), which could result in prodrug activation and absorption into proximal tissues from the circulation. Hydrolysis of the prodrugs in mouse plasma *ex vivo* confirms that prodrug activation does occur in the circulation. However, this model would predict that there would be nearly equimolar concentrations of active drug in all tissues if it were the dominant mechanism. Both the lung and spleen, two highly perfused organs, have significantly lower concentrations of active drug than do many of the other tissues analyzed, suggesting this does not account for the majority of prodrug activation observed.

Concentrations of active drug present in peripheral tissues from mice treated with the non-FAP cleavable prodrug controls can be used as an indicator of specificity. Examination of skeletal muscle demonstrated that ≥80% of the active drug generated from the ERGETGP-S12ADT prodrug may be specific for FAP activity *in vivo*. Therefore, a portion of the active drug in non-target tissues may be due to non-specific activation, suggesting that enhanced tumor-selective accumulation may be achieved through further refinement of the cleavage sequence.

A third explanation for the wide tissue distribution is likely due to FAP's broader expression pattern than was previously appreciated. FAP is now known to be expressed by mesenchymal stem cells (MSC), which have recently been identified at low levels in tissues throughout the body as part of normal homeostatic mechanisms (16). MSCs have significant immunomodulatory properties and traffic to sites of inflammation where they play a role in mediating the immune response. MSCs have also been shown to traffic to sites of cancer due to the high levels of cytokines and chemokines expressed and have been identified in primary prostatectomy tissue prior to *ex vivo* expansion using multi-parameter flow cytometry (16,36). MSCs are a significant source of CAFs in the cancer microenvironment (16,37), which may explain the increased accumulation of active drug in tumor tissue. Recent data suggests that FAP is also expressed by TAMs (17), which could contribute to drug activation and accumulation in the tumor as well. Independent of the cell-type driving drug activation in the tumor, low level expression of FAP on these cells in normal tissues likely contributes to the biodistribution pattern observed for the active drug.

Even so, treatment with a FAP-activated prodrug resulted in a significant inhibition of tumor growth in both breast and prostate cancer xenograft models. Dose intensification (3 cycles) did result in the death of one animal for reasons that could not be determined, but no mortality was observed in any of the animals (>70 to date) treated on a dosing regimen consisting of three consecutive daily doses (6.8 mg/kg/dose) for 1–2 cycles. Furthermore, the ERGETGP-S12ADT FAP-activated prodrug is nearly equivalent to docetaxel in its ability to abrogate LNCaP xenograft growth. Impressively, this comparable therapeutic effect is observed with only one-fourth the standard administered dose of docetaxel on a molar basis (10 vs. 40 nmoles, respectively).

Docetaxel is a widely-used chemotherapeutic agent in the treatment of multiple malignancies, including breast cancer, non-small cell lung cancer (NSCLC), and castration-resistant metastatic prostate cancer (38). The widespread use of docetaxel in the clinical setting occurs despite well-known side effects and toxicity associated with its dispensation

to patients (39–41). Mice treated with docetaxel routinely suffer and sustain as much as a 30% loss in their total body weight under standard therapeutic regimens in our laboratory. Weight loss following therapy is commonly used as an indicator of drug-induced toxicity with changes greater than 10–15% frequently seen as impacting quality-of-life. This is in contrast to animals treated with a FAP-activated prodrug who lose <15% of their body weight post-therapy and return to their pre-treatment weight within 1 week, suggesting that any toxicity that does occur is rapidly reversed. A point further highlighted by the lack of any discernible histopathological differences in tissues from treated and untreated animals at 20 days post-therapy.

Recent studies have demonstrated that elimination of FAP-positive cells using genetic engineering techniques or FAP-targeted T-cells restores host immunological control of tumor growth (19,42). Unfortunately, deletion of this cell population using these methods can also lead to fatigue, cachexia, anemia, and severe defects in hematopoiesis (31–32). These data suggested that FAP-targeted therapies would face potentially insurmountable side effects in their clinical development. In contrast, a second FAP-targeted chimeric antigen receptor (CAR) being developed by an independent group observed no such toxicity in their preclinical models (42). The reason for this discrepancy in toxicity between two seemingly comparable immunotherapies is unclear, but may be related to the epitope targeted by the scFv used in each of the constructs (42). In the latter case, this selectively leads to deletion of cells that highly overexpress FAP, but not their low expressing counterparts (42). The lack of any severe toxicity observed in the latter study and our work highlights the differences between total ablation of all FAP-positive cells in a host using genetic models and the elimination of subsets of FAP-expressing cells as is likely to be achieved using prodrugs and other clinically-relevant therapies. Additionally, the importance of pharmacokinetics and the damage response in normal tissue cannot be overstated in mitigating potential toxicity. As demonstrated in the current study, tumor-selective accumulation, rapid clearance from circulation, and the ability of normal tissues to repair low levels of damage can be key factors in minimizing drug-induced toxicity while maintaining a therapeutic response.

Importantly, the studies described above were performed in immunocompetent hosts and the anti-tumor effects were at least partially mediated through stimulation of endogenous CD8+ T-cell effector functions (42). The role of FAP-positive cells as central mediators of immunosurveillance implicates MSCs as primary targets driving the anti-tumor response in these models and suggests other approaches targeting this population may also be of clinical benefit. Notably, the current study is performed in immunocompromised animals, suggesting there can be a non-immune mediated component to the anti-tumor effect of FAP-targeted therapies as well. This may be the result of a prodrug-induced bystander effect (i.e., molecular grenades (2)), such as the one described herein (9), or through effects directly on the stroma itself. The stroma is a key component of many tumors and disrupting it can have significant effects on tumor growth, survival, metastatic dissemination and colonization; independent of any effects on the immune system (10,16). The level of stromal dependence likely varies both across tumor types and between tumors originating in the same tissue as a function of stage and their molecular profile. Additionally, it is unclear how this dependence correlates with the amount of stroma present. Future studies using these FAP-activated

prodrugs in immunocompetent hosts would be of great interest to determine if synergistic effects could be achieved through direct targeting of the stroma, indirect effects on adjacent cells through a bystander effect, and enhanced immunosurveillance.

In summary, a FAP-activated prodrug with significant anti-tumor efficacy against both breast and prostate cancer xenograft models has been generated. The pharmacokinetics of a FAP-selective prodrug and its activation have been characterized in mice receiving therapeutic doses with no treatment-associated toxicity by histopathologic standards. Further refinement of the FAP-selective cleavage sequence to improve specificity may be warranted to extend the therapeutic window and reduce activation in non-target tissues. Overall, these studies justify the continued development of FAP-targeted prodrugs as potential pan-tumor therapeutic agents.

Acknowledgments

The authors would like to acknowledge the following funding sources: Prostate Cancer Foundation (PCF) Young Investigator Award (to WNB), NIH grant (5RO1CA124764) and Susan B Komen Grant (to SRD), and NCI Prostate SPORE grant (P50CA58236 to SRD and JTI).

References

1. Vogelstein B, Papadopoulos N, Velculescu VE, Zhou S, Diaz LA Jr, Kinzler KW. Cancer genome landscapes. Science. 2013; 339(6127):1546–1558. [PubMed: 23539594]
2. Denmeade SR, Isaacs JT. Engineering enzymatically activated "molecular grenades" for cancer. Oncotarget. 2012; 3(7):666–667. [PubMed: 22837432]
3. Denmeade SR, Isaacs JT. The SERCA pump as a therapeutic target: making a "smart bomb" for prostate cancer. Cancer Biol Ther. 2005; 4(1):14–22. [PubMed: 15662118]
4. Denmeade SR, Jakobsen CM, Janssen S, Khan SR, Garrett ES, Lilja H, Christensen SB, Isaacs JT. Prostate-specific antigen-activated thapsigargin prodrug as targeted therapy for prostate cancer. J Natl Cancer Inst. 2003; 95(13):990–1000. [PubMed: 12837835]
5. Janssen S, Rosen DM, Ricklis RM, Dionne CA, Lilja H, Christensen SB, Isaacs JT, Denmeade SR. Pharmacokinetics, biodistribution, and antitumor efficacy of a human glandular kallikrein 2 (hK2)-activated thapsigargin prodrug. Prostate. 2006; 66(4):358–368. [PubMed: 16302271]
6. Denmeade SR, Mhaka AM, Rosen DM, Brennen WN, Dalrymple S, Dach I, Olesen C, Gurel B, Demarzo AM, Wilding G, Carducci MA, Dionne CA, Moller JV, Nissen P, Christensen SB, Isaacs JT. Engineering a prostate-specific membrane antigen-activated tumor endothelial cell prodrug for cancer therapy. Sci Transl Med. 2012; 4(140):140ra186.
7. Denmeade SR, Egerdie B, Steinhoff G, Merchant R, Abi-Habib R, Pommerville P. Phase 1 and 2 studies demonstrate the safety and efficacy of intraprostatic injection of PRX302 for the targeted treatment of lower urinary tract symptoms secondary to benign prostatic hyperplasia. Eur Urol. 2011; 59(5):747–754. [PubMed: 21129846]
8. Williams SA, Merchant RF, Garrett-Mayer E, Isaacs JT, Buckley JT, Denmeade SR. A prostate-specific antigen-activated channel-forming toxin as therapy for prostatic disease. J Natl Cancer Inst. 2007; 99(5):376–385. [PubMed: 17341729]
9. Brennen WN, Rosen DM, Wang H, Isaacs JT, Denmeade SR. Targeting carcinoma-associated fibroblasts within the tumor stroma with a fibroblast activation protein-activated prodrug. J Natl Cancer Inst. 2012; 104(17):1320–1334. [PubMed: 22911669]
10. Brennen WN, Isaacs JT, Denmeade SR. Rationale behind targeting fibroblast activation protein-expressing carcinoma-associated fibroblasts as a novel chemotherapeutic strategy. Mol Cancer Ther. 2012; 11(2):257–266. [PubMed: 22323494]
11. Rettig WJ, Garin-Chesa P, Healey JH, Su SL, Ozer HL, Schwab M, Albino AP, Old LJ. Regulation and heteromeric structure of the fibroblast activation protein in normal and transformed cells of

mesenchymal and neuroectodermal origin. Cancer Res. 1993; 53(14):3327–3335. [PubMed: 8391923]

12. Levy MT, McCaughan GW, Abbott CA, Park JE, Cunningham AM, Muller E, Rettig WJ, Gorrell MD. Fibroblast activation protein: a cell surface dipeptidyl peptidase and gelatinase expressed by stellate cells at the tissue remodelling interface in human cirrhosis. Hepatology. 1999; 29(6):1768–1778. [PubMed: 10347120]
13. O'Brien P, O'Connor BF. Seprase: an overview of an important matrix serine protease. Biochim Biophys Acta. 2008; 1784(9):1130–1145. [PubMed: 18262497]
14. Bauer S, Jendro MC, Wadle A, Kleber S, Stenner F, Dinser R, Reich A, Faccin E, Godde S, Dinges H, Muller-Ladner U, Renner C. Fibroblast activation protein is expressed by rheumatoid myofibroblast-like synoviocytes. Arthritis Res Ther. 2006; 8(6):R171. [PubMed: 17105646]
15. Acharya PS, Zukas A, Chandan V, Katzenstein AL, Pure E. Fibroblast activation protein: a serine protease expressed at the remodeling interface in idiopathic pulmonary fibrosis. Hum Pathol. 2006; 37(3):352–360. [PubMed: 16613331]
16. Brennen WN, Denmeade SR, Isaacs JT. Mesenchymal stem cells as a vector for the inflammatory prostate microenvironment. Endocr Relat Cancer. 2013; 20(5):R269–R290. [PubMed: 23975882]
17. Tchou J, Zhang PJ, Bi Y, Satija C, Marjumdar R, Stephen TL, Lo A, Chen H, Mies C, June CH, Conejo-Garcia J, Pure E. Fibroblast activation protein expression by stromal cells and tumor-associated macrophages in human breast cancer. Hum Pathol. 2013; 44(11):2549–2557. [PubMed: 24074532]
18. Fearon DT. The carcinoma-associated fibroblast expressing fibroblast activation protein and escape from immune surveillance. Cancer Immunol Res. 2014; 2(3):187–193. [PubMed: 24778314]
19. Kraman M, Bambrough PJ, Arnold JN, Roberts EW, Magiera L, Jones JO, Gopinathan A, Tuveson DA, Fearon DT. Suppression of antitumor immunity by stromal cells expressing fibroblast activation protein-alpha. Science. 2010; 330(6005):827–830. [PubMed: 21051638]
20. Rosenblum JS, Kozarich JW. Prolyl peptidases: a serine protease subfamily with high potential for drug discovery. Curr Opin Chem Biol. 2003; 7(4):496–504. [PubMed: 12941425]
21. Aggarwal S, Brennen WN, Kole TP, Schneider E, Topaloglu O, Yates M, Cotter RJ, Denmeade SR. Fibroblast activation protein peptide substrates identified from human collagen I derived gelatin cleavage sites. Biochemistry. 2008; 47(3):1076–1086. [PubMed: 18095711]
22. Christiansen VJ, Jackson KW, Lee KN, McKee PA. Effect of fibroblast activation protein and alpha2-antiplasmin cleaving enzyme on collagen types I, III, and IV. Arch Biochem Biophys. 2007; 457(2):177–186. [PubMed: 17174263]
23. Lebeau AM, Brennen WN, Aggarwal S, Denmeade SR. Targeting the cancer stroma with a fibroblast activation protein-activated promelittin protoxin. Mol Cancer Ther. 2009
24. Christensen SB, Skytte DM, Denmeade SR, Dionne C, Moller JV, Nissen P, Isaacs JT. A Trojan horse in drug development: targeting of thapsigargins towards prostate cancer cells. Anticancer Agents Med Chem. 2009; 9(3):276–294. [PubMed: 19275521]
25. Jakobsen CM, Denmeade SR, Isaacs JT, Gady A, Olsen CE, Christensen SB. Design, synthesis, and pharmacological evaluation of thapsigargin analogues for targeting apoptosis to prostatic cancer cells. J Med Chem. 2001; 44(26):4696–4703. [PubMed: 11741487]
26. Singh P, Mhaka AM, Christensen SB, Gray JJ, Denmeade SR, Isaacs JT. Applying linear interaction energy method for rational design of noncompetitive allosteric inhibitors of the sarco- and endoplasmic reticulum calcium-ATPase. J Med Chem. 2005; 48(8):3005–3014. [PubMed: 15828839]
27. Vander Griend DJ, Antony L, Dalrymple SL, Xu Y, Christensen SB, Denmeade SR, Isaacs JT. Amino acid containing thapsigargin analogues deplete androgen receptor protein via synthesis inhibition and induce the death of prostate cancer cells. Mol Cancer Ther. 2009
28. Niedermeyer J, Scanlan MJ, Garin-Chesa P, Daiber C, Fiebig HH, Old LJ, Rettig WJ, Schnapp A. Mouse fibroblast activation protein: molecular cloning, alternative splicing and expression in the reactive stroma of epithelial cancers. Int J Cancer. 1997; 71(3):383–389. [PubMed: 9139873]

29. Niedermeyer J, Kriz M, Hilberg F, Garin-Chesa P, Bamberger U, Lenter MC, Park J, Viertel B, Puschner H, Mauz M, Rettig WJ, Schnapp A. Targeted disruption of mouse fibroblast activation protein. Mol Cell Biol. 2000; 20(3):1089–1094. [PubMed: 10629066]
30. Lee KN, Jackson KW, Christiansen VJ, Lee CS, Chun JG, McKee PA. Antiplasmin-cleaving enzyme is a soluble form of fibroblast activation protein. Blood. 2006; 107(4):1397–1404. [PubMed: 16223769]
31. Roberts EW, Deonarine A, Jones JO, Denton AE, Feig C, Lyons SK, Espeli M, Kraman M, McKenna B, Wells RJ, Zhao Q, Caballero OL, Larder R, Coll AP, O'Rahilly S, Brindle KM, Teichmann SA, Tuveson DA, Fearon DT. Depletion of stromal cells expressing fibroblast activation protein-alpha from skeletal muscle and bone marrow results in cachexia and anemia. J Exp Med. 2013; 210(6):1137–1151. [PubMed: 23712428]
32. Tran E, Chinnasamy D, Yu Z, Morgan RA, Lee CC, Restifo NP, Rosenberg SA. Immune targeting of fibroblast activation protein triggers recognition of multipotent bone marrow stromal cells and cachexia. J Exp Med. 2013; 210(6):1125–1135. [PubMed: 23712432]
33. Davidson GA, Varhol RJ. Kinetics of thapsigargin-Ca(2+)-ATPase (sarcoplasmic reticulum) interaction reveals a two-step binding mechanism and picomolar inhibition. J Biol Chem. 1995; 270(20):11731–11734. [PubMed: 7744817]
34. Thastrup O, Cullen PJ, Drobak BK, Hanley MR, Dawson AP. Thapsigargin, a tumor promoter, discharges intracellular Ca2+ stores by specific inhibition of the endoplasmic reticulum Ca2(+)-ATPase. Proc Natl Acad Sci U S A. 1990; 87(7):2466–2470. [PubMed: 2138778]
35. Christensen SB, Andersen A, Kromann H, Treiman M, Tombal B, Denmeade S, Isaacs JT. Thapsigargin analogues for targeting programmed death of androgen-independent prostate cancer cells. Bioorg Med Chem. 1999; 7(7):1273–1280. [PubMed: 10465403]
36. Brennen WN, Chen S, Denmeade SR, Isaacs JT. Quantification of Mesenchymal Stem Cells (MSCs) at sites of human prostate cancer. Oncotarget. 2013; 4(1):106–117. [PubMed: 23362217]
37. Mishra PJ, Humeniuk R, Medina DJ, Alexe G, Mesirov JP, Ganesan S, Glod JW, Banerjee D. Carcinoma-associated fibroblast-like differentiation of human mesenchymal stem cells. Cancer Res. 2008; 68(11):4331–4339. [PubMed: 18519693]
38. Montero A, Fossella F, Hortobagyi G, Valero V. Docetaxel for treatment of solid tumours: a systematic review of clinical data. Lancet Oncol. 2005; 6(4):229–239. [PubMed: 15811618]
39. Chan S. Docetaxel vs doxorubicin in metastatic breast cancer resistant to alkylating chemotherapy. Oncology (Williston Park). 1997; 11 Suppl 8(8):19–24. [PubMed: 9364537]
40. Engels FK, Verweij J. Docetaxel administration schedule: from fever to tears? A review of randomised studies. Eur J Cancer. 2005; 41(8):1117–1126. [PubMed: 15911234]
41. Kintzel PE, Michaud LB, Lange MK. Docetaxel-associated epiphora. Pharmacotherapy. 2006; 26(6):853–867. [PubMed: 16716138]
42. Wang LC, Lo A, Scholler J, Sun J, Majumdar RS, Kapoor V, Antzis M, Cotner CE, Johnson LA, Durham AC, Solomides CC, June CH, Pure E, Albelda SM. Targeting Fibroblast Activation Protein in Tumor Stroma with Chimeric Antigen Receptor T Cells Can Inhibit Tumor Growth and Augment Host Immunity without Severe Toxicity. Cancer Immunol Res. 2014; 2(2):154–166. [PubMed: 24778279]

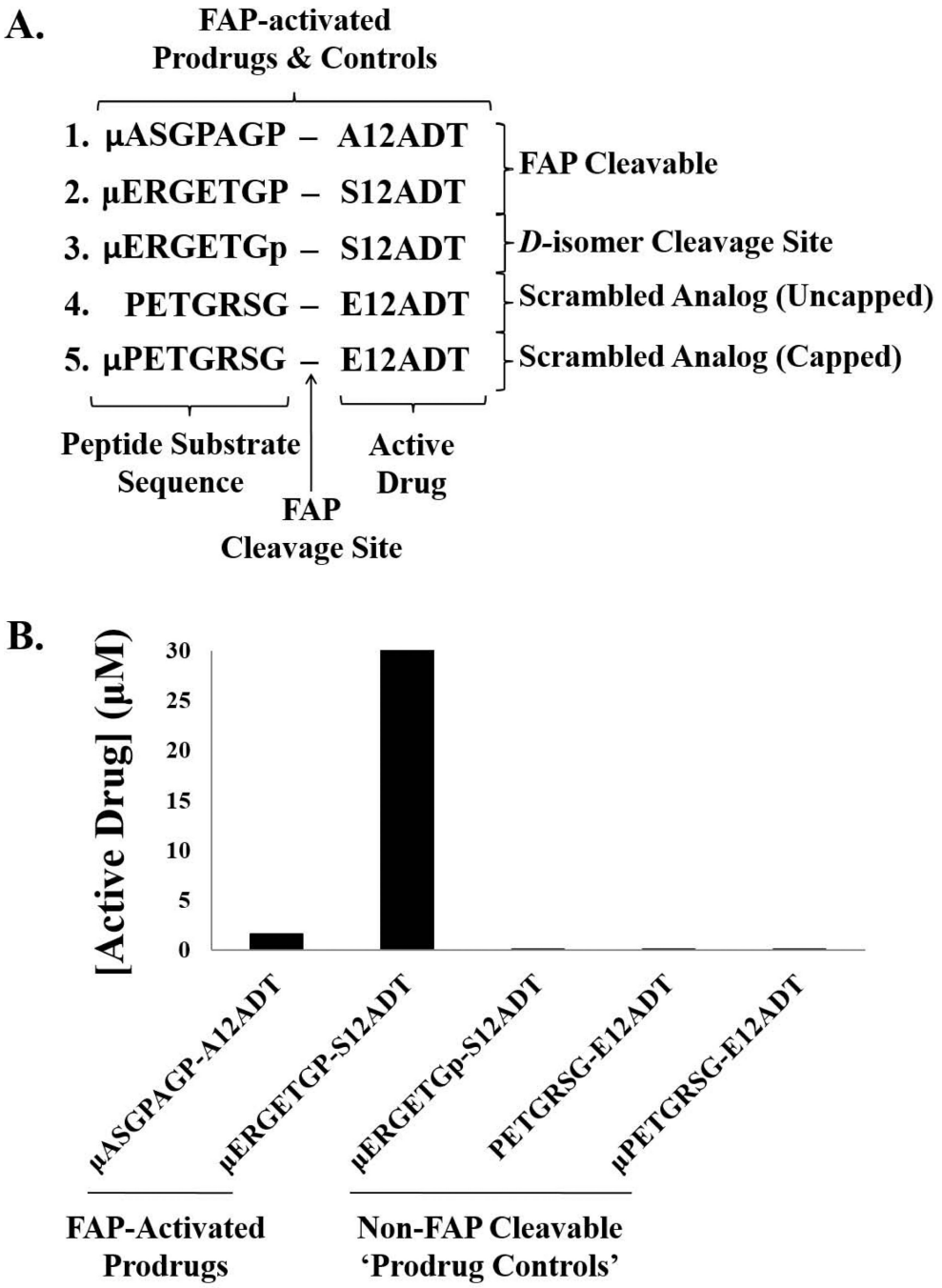

Figure 1.

Design and characterization of FAP-activated prodrugs and analog controls. **(A)** Design of FAP-activated prodrugs and their non-FAP cleavable analog controls. **(B)** FAP-mediated activation of prodrugs *ex vivo*. The active form of the drugs (A- or S-12ADT, respectively) were produced from both FAP-cleavable prodrugs (ASGPAGP-A12ADT and ERGETGP-S12ADT), but not from the non-FAP cleavable prodrug analogs. (p) represents the *D*-isomer of proline and (µ) represents morpholino-cap on the NH_2-terminus of the prodrug peptide sequence.

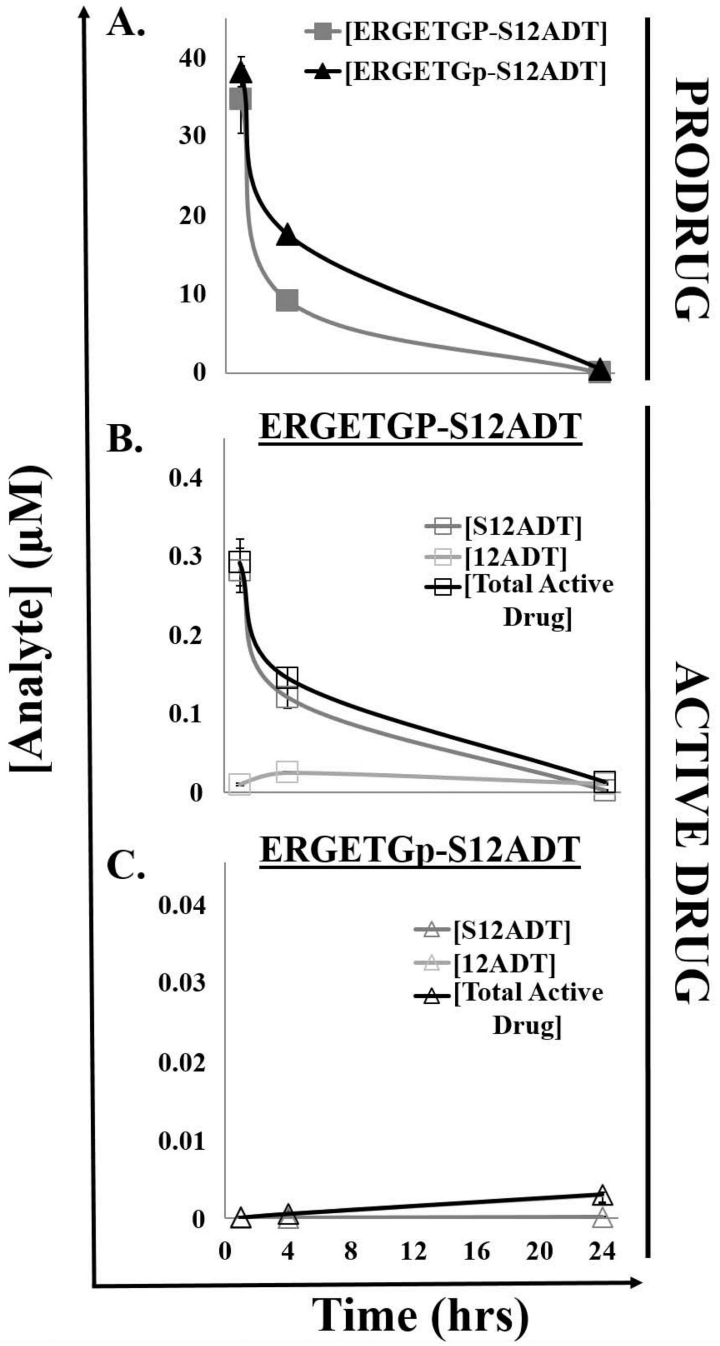

Figure 2.

Pharmacokinetics of FAP-selective prodrug activation in plasma from tumor-bearing hosts. **(A)**The half-life ($t_{1/2}$) of the full-length FAP-activated ERGETGP-S12ADT prodrug and *D*-isomer control in mouse plasma is ~4–5 hrs after reaching a peak concentration (C_{max}) of 35–40 μM *in vivo*. **(B)** Production of the active form of the drug from the full-length ERGETGP-S12ADT prodrug in mouse plasma *in vivo*. Less than 1% of the prodrug is converted to the active form in plasma. The total active drug produced includes both the S12ADTand 12ADT forms. **(C)** Production of the active form of the drug from the non-FAP

cleavable ERGETGp-S12ADT *D*-isomer control. S12ADT was not generated; however, low levels of 12ADT were detected (<0.01% of total administered dose). Error bars represent +/− standard error.

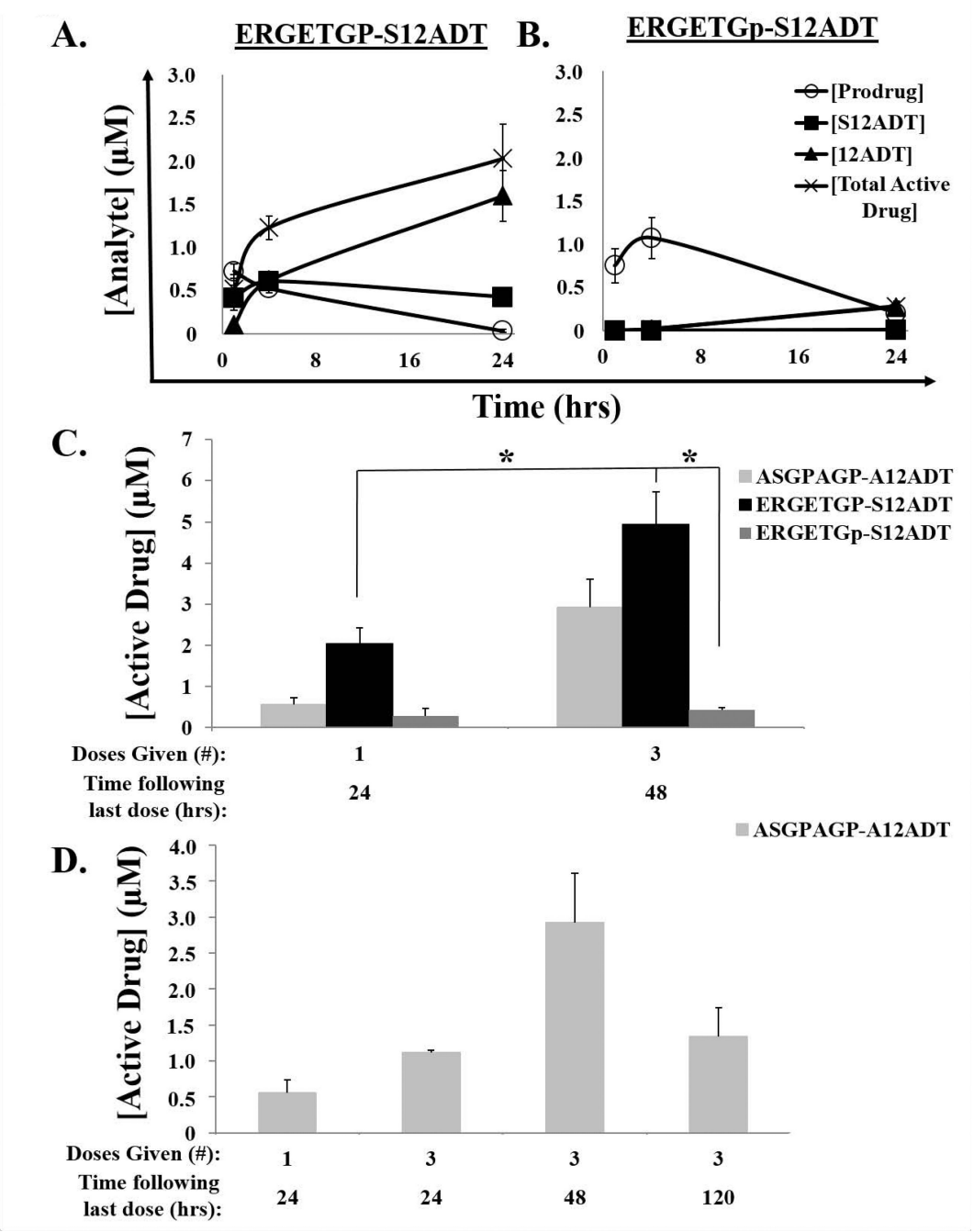

Figure 3.

Pharmacokinetics of FAP-selective prodrug activation in tumors from immunocompromised murine hosts bearing MCF-7 human breast cancer xenografts. **(A)** Half-life ($t_{1/2}$) of the full-length form of the FAP-activated ERGETGP-S12ADT prodrug in tumors is ~12 hrs; however, the active form of the drug (S12ADT + 12ADT) continues to accumulate and reaches concentrations of ~2 μM within 24 hrs. **(B)** The half-life of the non-FAP cleavable *D*-isomer analog, ERGETGp-S12ADT, is ~16 hrs in tumors. Similar to the plasma, only 12ADT is detectable in these tumors. Total active drug concentrations are ~7-fold lower

than those generated from the FAP-activated prodrug. **(C)** Active drug (S12ADT + 12ADT) accumulates in tumors following multiple doses (n = 3) reaching concentrations of ~5 μM with ERGETGP-S12ADT. **(D)** High concentrations (μM) of active drug (S12ADT + 12ADT) persist over time (≥5 days) in tumors following cessation of therapy. Error bars represent +/− standard error. P-values ≤ 0.05 (*) are considered statistically significant.

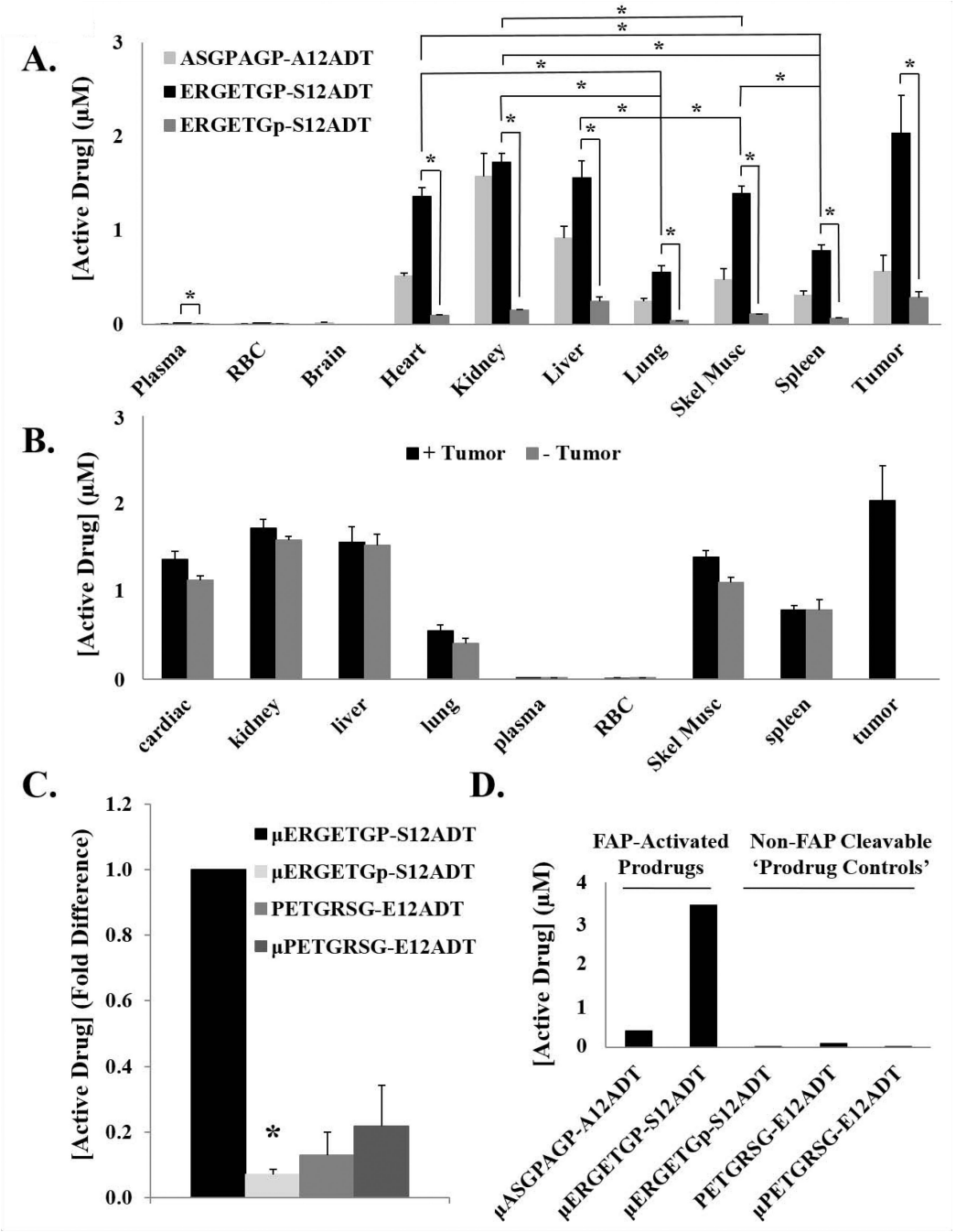

Figure 4.

Biodistribution of FAP-selective prodrug activation. **(A)** The concentrations of active drug (aa12ADT + 12ADT) produced from two FAP-activated prodrugs and the non-FAP cleavable *D*-isomer control were measured by LCMS in a panel of tissues from murine hosts bearing MCF-7 xenografts 24 hrs after a single IV dose. The greatest accumulation of active drug (S12ADT + 12ADT) from the full-length ERGETGP-S12ADT prodrug was detected in the tumor; however, high levels were also present in many of the non-target tissues analyzed. Experiment was performed in triplicate and error bars represent standard error.

Drug levels were not determined for the brain in animals treated with ERGETGP-S12ADT or ERGETGp-S12ADT. **(B)** Active drug concentrations (aa12ADT + 12ADT) in non-target tissues from tumor-bearing and naïve mice were not significantly different. Experiment was performed in triplicate. **(C)** Active drug concentrations (aa12ADT + 12ADT) present in skeletal muscle as a representative non-target tissue to measure non-specific activation of the prodrugs. Less than 10% of the amount of active drug detected in the skeletal muscle of mice treated with the full-length FAP-activated prodrug was found in those treated with the *D*-isomer analog. Active drug generated from the capped and non-capped scrambled analogs were approximately 15% and 20%, respectively, of that produced from the FAP-activated prodrug. Experiment was performed in triplicate. **(D)** Production of active drug (aa12ADT + 12ADT) from FAP-activated prodrugs and controls in mouse plasma *ex vivo*. Significant amounts of active drug were generated from the FAP-activated prodrugs, while substantially lower concentrations were produced from the non-FAP cleavable analog controls. Active drug includes aa12ADT + 12ADT in all panels. P-values ≤ 0.05 (*) are considered statistically significant. Error bars represent standard error

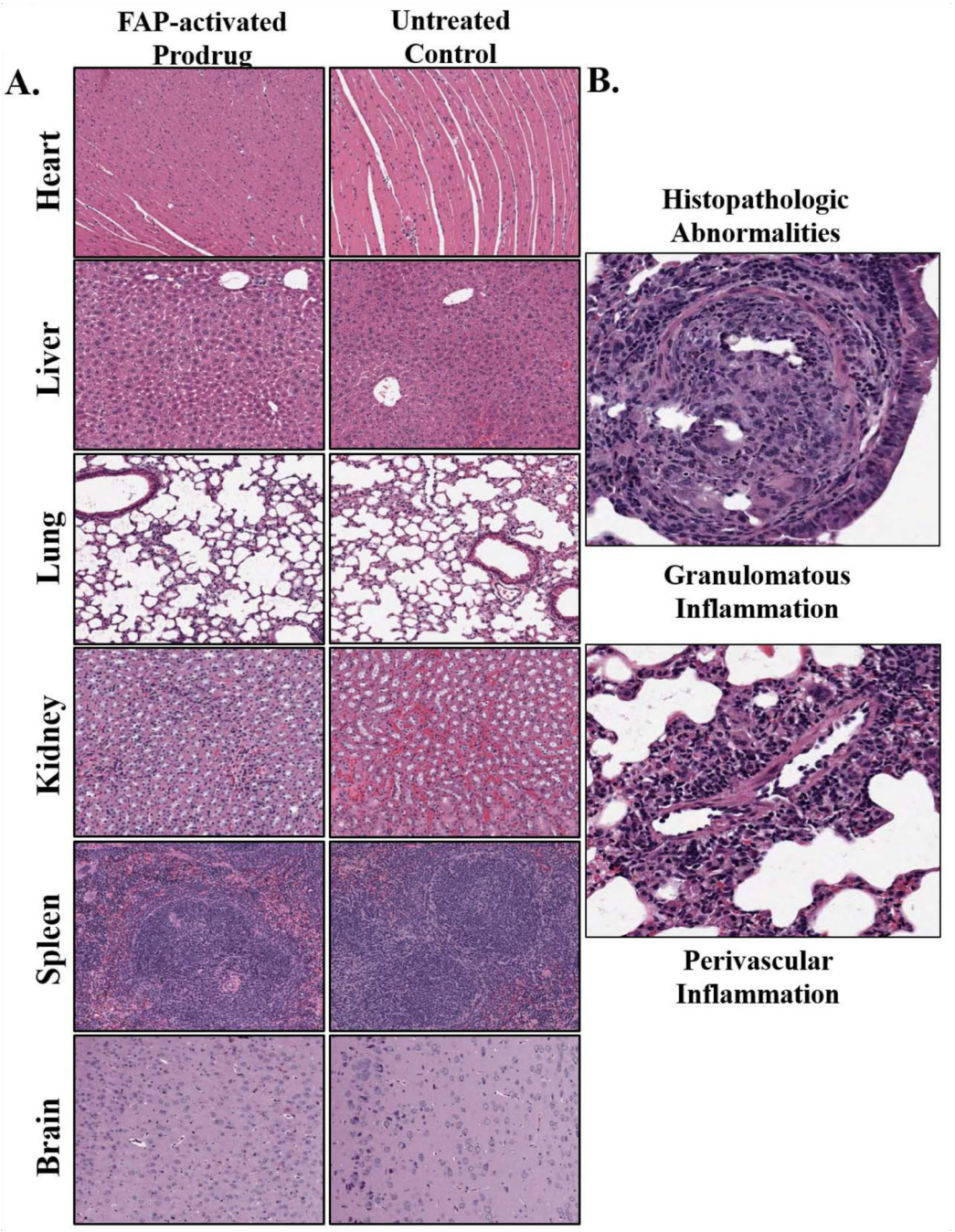

Figure 5.

Histopathologic analysis of tissues for assessment of drug-induced toxicity. **(A)** Animals received three daily IV doses of the FAP-activated ERGETGP-S12ADT prodrug and tissues were harvested 20 days post-therapy for comparison to vehicle-treated controls. All tissues were examined in a blinded fashion and no differences could be detected between control and treated animals. All tissues were considered histopathologically normal. Three animals per group were examined and images are representative of a typical 10× field. **(B)** The only abnormal pathology observed was a single granuloma with mild inflammation in the lung of

a single treated animal. Small granuloma (*upper panel*) along with moderate perivascular inflammation marked by the presence of lymphocytes and macrophages (*lower panel*). This event was considered unrelated to therapy as they only occurred in a single animal and no evidence of apoptotic cells or other drug-related mechanisms of action were observed. Images were taken at 20×.

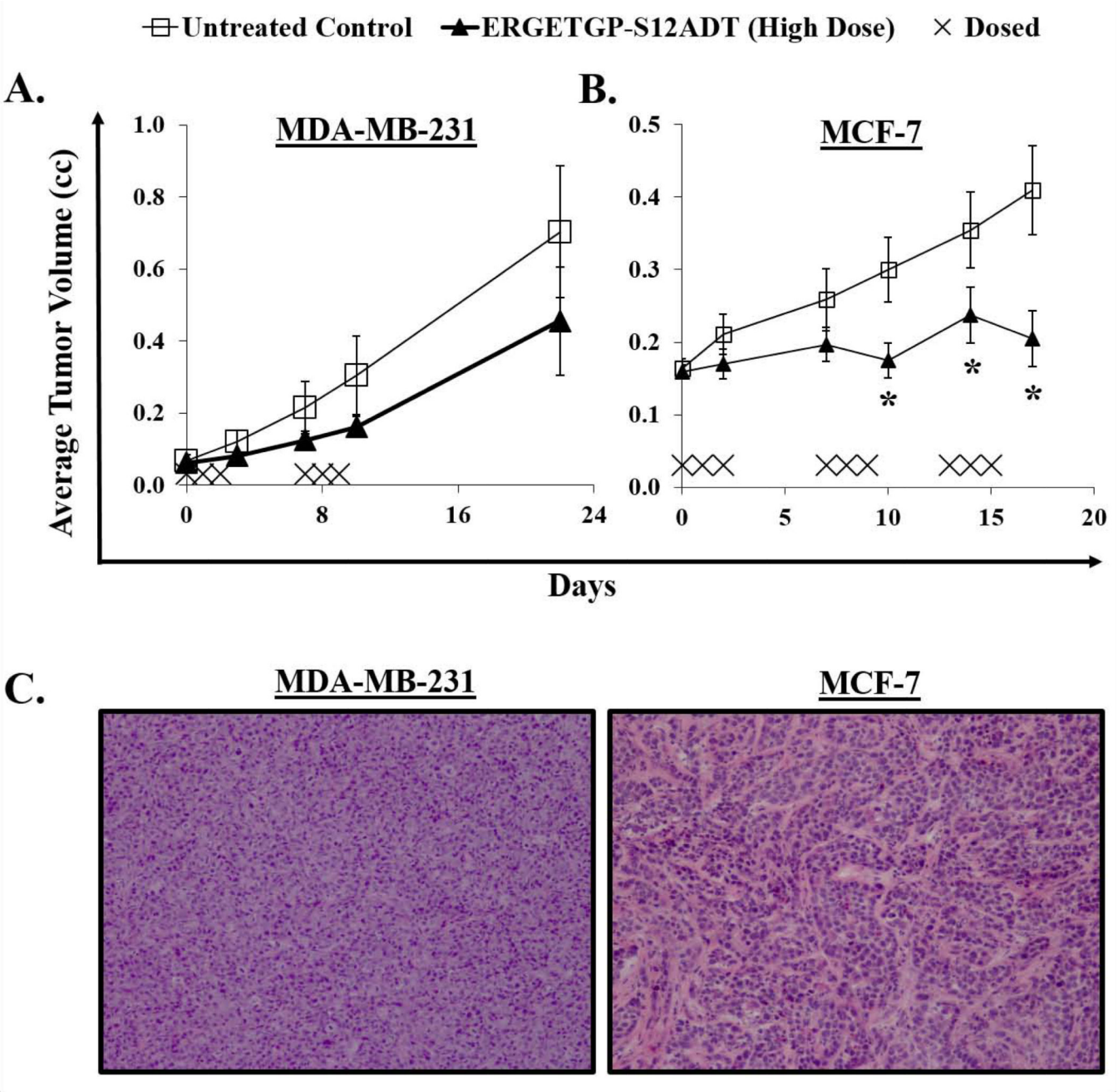

Figure 6.

Efficacy of the FAP-activated ERGETGP-S12ADT prodrug against human breast cancer xenograft models. **(A)** Animals bearing MDA-MB-231 xenografts were treated with three consecutive daily IV doses for 2 cycles initiated on a one week interval (days 0 and 7). While therapy showed a modest anti-tumor effect, this was not significantly different from vehicle-treated controls. **(B)** A significant inhibition of tumor growth was observed against MCF-7 xenografts in mice treated with the FAP-activated prodrug. Animals were received 3 cycles of 3 consecutive daily doses with a one week interval between cycle initiation (i.e., days 0, 7, and 13). **(C)** Representative H&E staining from MDA-MB-231 (*left panel)* and

MCF-7 (*right* panel) breast cancer xenografts. Images taken at 10× magnification. Error bars represent +/− standard error. P-values ≤ 0.05 (*) are considered statistically significant.

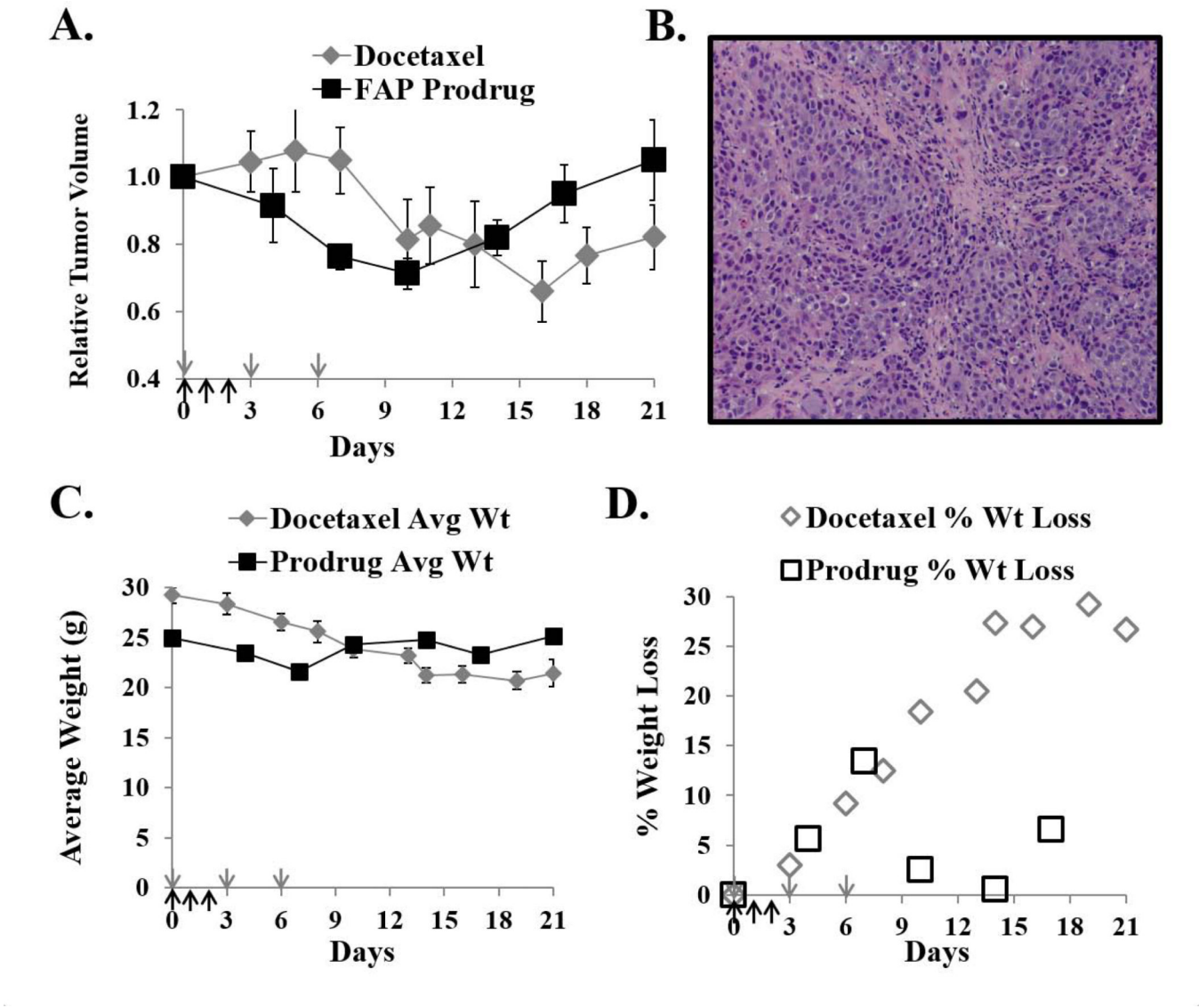

Figure 7.

Comparison of efficacy and toxicity of a FAP-activated prodrug to docetaxel. **(A)** The FAP-activated ERGETGP-S12ADT prodrug has comparable efficacy against LNCaP human prostate cancer xenografts as a standard chemotherapeutic agent, docetaxel. The docetaxel group received 40 nmoles IV on days 0, 3, 6 (grey arrows). The FAP-activated prodrug group received10 nmoles prodrug IV days 0, 1, 2 (black arrows). **(B)** Representative H&E staining from LNCaP prostate cancer xenografts. Image taken at 10× magnification. **(C)** Average body weight of animals from each treatment group. **(D)** Percent of total body weight lost in animals from each treatment group. Animals treated with docetaxel on this treatment regimen suffered and sustained substantially greater weight loss than did animals receiving the FAP-activated prodrug (30 vs. ≤ 15%, respectively) at nearly equipotent doses. Error bars represent +/− standard error.